

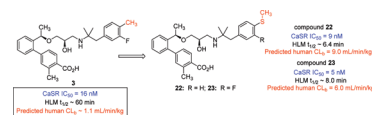
# Metabolism-Guided Design of Short-Acting Calcium-Sensing Receptor Antagonists

James A. Southers, Jonathan N. Bauman, David A. Price, Paul S. Humphries, Gayatri Balan, John F. Sagal, Tristan S. Maurer, Yan Zhang, Robert Oliver, Michael Herr, David R. Healy, Mei Li, Brendon Kapinos, Gwendolyn D. Fate, Keith A. Riccardi, Vishwas M. Paralkar, Thomas A. Brown, and Amit S. Kalgutkar\*

Pfizer Global Research and Development, Groton, Connecticut 06340

**ABSTRACT** As part of a strategy to deliver short-acting calcium-sensing receptor (CaSR) antagonists, the metabolically labile thiomethyl functionality was incorporated into the zwitterionic amino alcohol derivative **3** with the hope of increasing human clearance through oxidative metabolism, while delivering a pharmacologically inactive sulfoxide metabolite. The effort led to the identification of thioanisoles **22** and **23** as potent and orally active CaSR antagonists with a rapid onset of action and short pharmacokinetic half-lives, which led to a rapid and transient stimulation of parathyroid hormone in a dose-dependent fashion following oral administration to rats. On the basis of the balance between target pharmacology, safety, and human disposition profiles, **22** and **23** were advanced as clinical candidates for the treatment of osteoporosis.

**KEYWORDS** Calcium, CaSR antagonists, PTH, cytochrome P450, metabolite, oxidation



Osteoporosis affects a substantial proportion of the elderly population and causes notable morbidity, deterioration in quality of life, and mortality due to associated fragility fractures.<sup>1</sup> Agents for the treatment of osteoporosis are classified as either antiresorptive or anabolic. While antiresorptive agents (e.g., bisphosphonates and estrogen) prevent further bone loss, they cause relatively small increases in bone formation. In contrast, anabolic agents act by stimulating osteoblast function and new bone formation. The only anabolic agent currently available in the United States is teriparatide (Forteo), a synthetic 1–34 amino acid peptide fragment of the human parathyroid hormone (PTH), which has been shown to increase bone mineral density (BMD) and reduce fracture rates in osteoporosis patients after daily subcutaneous administration.<sup>2</sup> A viable alternative to an injectible agent is the identification of a small molecule agent that would stimulate secretion of endogenously stored PTH from the parathyroid glands. PTH secretion is tightly regulated by the G-protein-coupled calcium-sensing receptor (CaSR) expressed on the surface of the parathyroid cells.<sup>3,4</sup> CaSR modulates circulating levels of calcium; a hypocalcemic state (low serum calcium concentrations) results in PTH release from the parathyroid glands, whereas increase in calcium suppresses the release of this hormone.<sup>3,4</sup> Small molecule CaSR antagonists replicate a hypocalcemic state and stimulate PTH release.<sup>4,5</sup> Pharmacodynamic (PD) studies with prototype CaSR antagonists such as NPS-2143 (Figure 1) reveal that the profile of PTH stimulation following CaSR antagonism must be rapid and

transient for bone anabolism since sustained activation causes prolonged PTH secretion and a catabolic state, such as hyperthyroidism.<sup>4,5</sup> To achieve such a PD effect, a CaSR antagonist must demonstrate rapid oral absorption and a short pharmacokinetic (PK) half-life ( $t_{1/2}$ ) of ~1 h [ideally achieved through a human blood clearance ( $CL_b$ ) and steady state distribution volume ( $V_{d,ss}$ ) of 10 mL/min/kg and 1 L/kg, respectively].<sup>6</sup>

A number of CaSR antagonists have been reported in the literature.<sup>6–9</sup> Results of phase 2A clinical trials have also been reported with ronacaleret (Figure 1) and JTT-305.<sup>10,11</sup> Despite a positive proof-of-concept in a 28 day study in postmenopausal women, a dose-ranging clinical trial of ronacaleret was discontinued due to poor effects on BMD.<sup>10</sup> While the reason(s) for lack of efficacy of ronacaleret remains unclear, confidence in the mechanism was restored shortly after the disclosure that JTT-305 significantly increased lumbar spine BMD in a 12 week clinical trial while showing favorable effects on markers of bone formation and resorption in patients with postmenopausal osteoporosis.<sup>11</sup> As such, the structure of JTT-305 is unknown but is believed to be in similar chemotype to that of ronacaleret.

Toward the pursuit of proprietary chemotypes, our laboratory recently disclosed a series of tricyclic zwitterionic amino

Received Date: April 8, 2010

Accepted Date: May 10, 2010

Published on Web Date: May 13, 2010

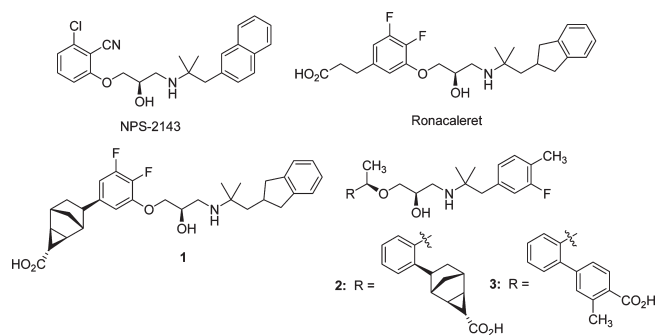


**Figure 1.** Structures of representative CaSR antagonists.

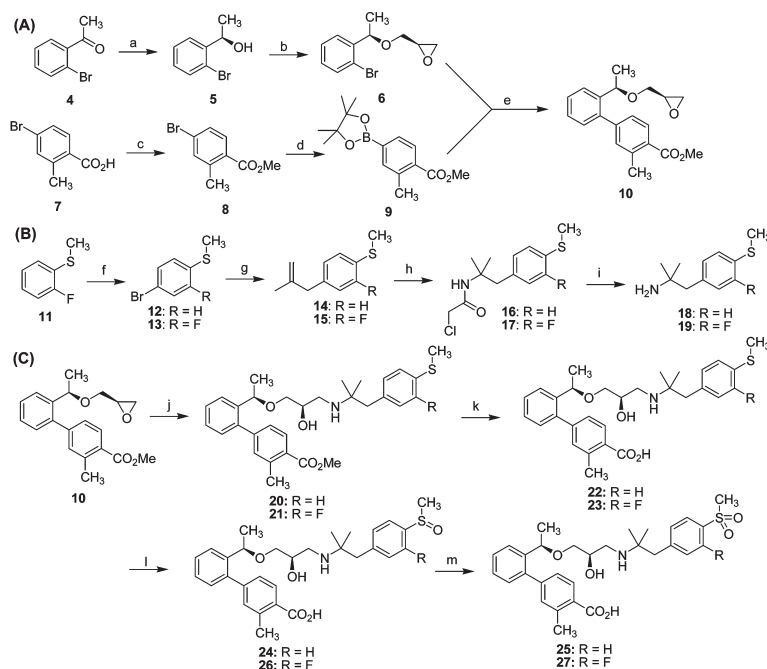
alcohol (e.g., **1** and **2**)-based CaSR antagonists (Figure 1).<sup>8</sup> While members within the series displayed requisite CaSR pharmacology, the projected low  $CL_b$  using human liver microsomes (HLM) for leads **1** and **2** was concerning. Consequently, we directed our attention to the optimization of the amino alcohol chemical space in search of compounds endowed with not only analogous pharmacologic properties but also improvements in human PK profiles. Comparison of the HLM stability of NPS-2143 with zwitterionic amino alcohols suggests that the carboxylic acid moiety significantly reduces lipophilicity, resulting in reduced affinity toward metabolism by cytochrome P450 (CYP) enzymes.<sup>8</sup> Metabolic profiling of several zwitterionic amino alcohols in HLM revealed trace amounts of hydroxylation on the 2-methylpropan-2-amine substituent (e.g., indanyl group in **1** and ronacaleret and 2-fluorotolyl motif in **2** and **3**<sup>12</sup>) to be a common and dominant metabolic fate. We reasoned that strategic placement of a metabolically labile functional group on the region predisposed to CYP metabolism would provide the necessary boost in metabolic clearance. For this assessment, we decided to focus our efforts on biaryl carboxylic acids (e.g., compound **3**, Figure 1) described in a patent application by Japan Tobacco.<sup>12</sup> From prior in-house experience in the selective serotonin (SER) reuptake inhibitor program,<sup>13</sup> we were aware that CYP-catalyzed thioalkyl *S*-oxidation can be an efficient and rapid metabolic process and therefore offered an attractive avenue of pursuit in the present situation. Herein, we describe our efforts to optimize the human disposition profile of **3** while maintaining primary CaSR pharmacology and selectivity, which resulted in the identification of clinical candidates **22** and **23**.

The synthesis of the common epoxide intermediate **10** is shown in Scheme 1A. Stereoselective reduction of 2-bromoacetophenone (**4**) with (+)-diisopinocampheyl chloroborane [(+)-DIP-Cl] generated the (*R*)-form of secondary alcohol **5** (> 98% ee),<sup>16</sup> which was reacted with glycidyl tosylate to afford bromo epoxide **6** in a 10:1 ratio of diastereomers. Palladium-catalyzed coupling of **6** with the pinacol boronate ester **8** afforded **10** as a viscous oil. Amines **18** and **19** were synthesized from the corresponding bromothioanisole derivatives **12** and **13**, respectively (Scheme 1B). Grignard formation in **12** and **13** followed by reaction with 3-chloro-2-methylpropene yielded olefins **14** and **15**, which were converted to chloroacetamide analogues **16** and **17**, respectively, via a Ritter reaction. Deprotection of **16** and/or **17** with thiourea in the presence of AcOH

furnished **18** and **19**, which were characterized as the corresponding hydrochloride salts. Lewis acid-mediated epoxide ring opening in **10** by **18** and/or **19** afforded **20** and **21**, respectively, which were hydrolyzed to title compounds **22** and **23**, respectively (Scheme 1C). Putative sulfoxide metabolites **24** and **26** were synthesized from the oxidation of **22** and **23** in the presence of *N*-bromosuccinimide. Oxidation of **22** and **23** in the presence of Oxone afforded corresponding sulfone **25** and **27** metabolites, respectively.

In vitro CaSR antagonist potency was examined using a fluorimetric imaging plate reader (FLIPR)-based assay, which measures the ability of test compounds to block increases in the concentration of cytoplasmic calcium in HEK293 cells expressing human CaSR. Ronacaleret and **3**, which were included as positive controls, revealed CaSR antagonist potency ( $IC_{50}$ ) values of 0.11 and 0.016  $\mu$ M, respectively. Compounds **22** and **23** were superior CaSR antagonists with  $IC_{50}$  values of 0.009 and 0.005  $\mu$ M, respectively. Selectivity against  $\alpha_{2\beta}$  and  $\beta_2$ -adrenergic receptor binding, human ether-a-go-go related gene (hERG), and CYP2D6 inhibition was also examined, given the association of such off-target pharmacologies with some amino alcohol-based CaSR antagonists.<sup>9</sup> In binding assays (Table 1), weak cross-reactivity with the  $\alpha_{2\beta}$  and  $\beta_2$  receptors and hERG ion current was noted with ronacaleret, **3**, **22**, and **23**. Competitive CYP2D6 inhibition was also observed with **3**, **22**, and **23** ( $IC_{50}$  = 1.3–3.7  $\mu$ M). In contrast, ronacaleret did not inhibit CYP2D6 activity ( $IC_{50}$  > 30  $\mu$ M). Because basic amino alcohols have been reported as inhibitors of several monoamine transporters,<sup>9</sup> ronacaleret, **3**, **22**, and **23** were tested for inhibition of SER, norepinephrine (NER), and dopamine (DA) transporters. Inhibitory effects against SERT ( $IC_{50}$  = 12–> 25  $\mu$ M), NERT ( $IC_{50}$  = 9.0–> 25  $\mu$ M), and DAT ( $IC_{50}$  = 4.0–4.5  $\mu$ M) by **3**, **22**, and **23** were generally weak in nature (Table 1). In contrast, ronacaleret appeared to possess significantly more potent interactions against SERT and DAT.

Pleased with the results of the in vitro pharmacologic evaluation and in particular with the >1000-fold selectivity over hERG, we focused our attention on the metabolism of **22** and **23** in HLM. The biotransformation pathways of **22** ( $MH^+$  = 508, panel A) and **23** ( $MH^+$  = 526, panel B) in NADPH-supplemented HLM were similar and consisted primarily of the sulfoxide metabolites **24** ( $MH^+$  = 524) and **26** ( $MH^+$  = 542), respectively (Figure 2). Further oxidation to the corresponding sulfones **25** ( $MH^+$  = 540) and **27** ( $MH^+$  = 558) was also detected as a minor metabolite fate. The metabolites were identified unambiguously via comparison of retention times and mass spectra with those of the authentic standards. For the success of our overall strategy, we knew that any (circulating) metabolite formed must be significantly less active than the parent to avoid sustained PTH stimulation. To our delight, both the sulfoxide and the sulfone metabolites of **22** and **23** were devoid of CaSR antagonism ( $IC_{50}$  values > 100  $\mu$ M). The potentially toxic mercaptan metabolite derived from thioanisole *S*-demethylation in **22** and **23** was not detected in HLM incubations. Finally, inclusion of CYP3A4 inhibitor ketoconazole in HLM incubations eliminated metabolite formation in **22** and **23**, implying that CYP3A4 was responsible for their biotransformation.

Scheme 1. Synthesis of Compounds **22** and **23**<sup>a</sup>

<sup>a</sup> Conditions: (a) (+)-DIP-chloride, THF,  $-25^{\circ}\text{C}$ , diethanolamine. (b) Toluene-4-sulfonic acid (*R*)-1-oxiranylmethyl ester, NaH, THF, DMF,  $0^{\circ}\text{C}$  to room temperature. (c) MeOH,  $\text{H}_2\text{SO}_4$ , reflux, 20 h. (d) Bis(Pinacolato)diboron, [1,1'-bis(diphenylphosphino)ferrocene] dichloropalladium(II), KOAc,  $80^{\circ}\text{C}$  and 3 h to room temperature and 16 h. (e) [1,1'-Bis(diphenylphosphino)ferrocene] dichloropalladium(II),  $\text{Na}_2\text{CO}_3$ , EtOH, reflux 3 h. (f)  $\text{Br}_2$ ,  $\text{CH}_2\text{Cl}_2$ ,  $0^{\circ}\text{C}$  to room temperature. (g) Mg, cat.  $\text{I}_2$ , CuI, 3-chloro-2-methylpropene  $0^{\circ}\text{C}$  to room temperature, aqueous  $\text{NH}_4\text{Cl}$ . (h) Chloroacetonitrile, AcOH,  $\text{H}_2\text{SO}_4$ ,  $0^{\circ}\text{C}$  to room temperature. (i) AcOH, EtOH,  $100^{\circ}\text{C}$ , 16 h. (j) Compound **18** or **19**, 1.1 equiv  $\text{LiClO}_4$ , toluene,  $50^{\circ}\text{C}$ , 16 h. (l) *N*-Bromosuccinimide, silica gel,  $\text{CH}_2\text{Cl}_2$ , room temperature. (m) Oxone, MeOH– $\text{H}_2\text{O}$ ,  $0^{\circ}\text{C}$  to room temperature.

Table 1. CaSR Potency and Selectivity Data

compd	$\text{IC}_{50}$ ( $\mu\text{M}$ ) <sup>a</sup>								
	CaSR FLIPR	$\alpha_{2\beta}$ binding	$\beta_2$ binding	Nav1.5 binding	hERG binding	CYP2D6	SERT binding	NER binding	DA binding
ronacaleret	0.11	9.0	> 30	> 30	23	> 30	0.19	3.6	1.4
<b>3</b>	0.016	2.2	6.8	> 30	19	2.5	> 25	> 25	4.0
<b>22</b>	0.009	8.2	10	> 30	14	3.7	14	18	4.4
<b>23</b>	0.005	6.0	10	> 30	7.0	1.3	12	9.0	4.5

<sup>a</sup>  $\text{IC}_{50}$  values are means of at least three independent experiments. CaSR  $\text{IC}_{50}$  values represent the average of 15–20 separate determinations.

Our next objective was human  $\text{CL}_b$  predictions for **22** and **23**. In NADPH-supplemented HLM, **22** and **23** rapidly degraded with  $t_{1/2}$  values of less than 10 min. Scale-up of the microsomal  $t_{1/2}$  data using the well-stirred model<sup>14</sup> provided a complementary range of predicted human  $\text{CL}_b$  values for **22** (6.0 mL/min/kg) and **23** (9.0 mL/min/kg) (Table 2). Ronacaleret and **3** were relatively more stable toward metabolism in HLM ( $t_{1/2} = 50$ –60 min) yielding  $\text{CL}_b$  values of  $\sim 1.0$  mL/min/kg. In vitro–in vivo correlation (IVIVC) studies were undertaken in the rat to increase confidence in human  $\text{CL}_b$  projections (Table 2). Following intravenous (iv) administration, in vivo  $\text{CL}_b$  values of ronacaleret, **3**, **22**, and **23** were 2.0–4.0-fold greater than the corresponding  $\text{CL}_b$  estimates from rat liver microsomes. While the higher  $\text{CL}_b$  values of **22** and **23** relative to **3** clearly reflect the success of our design strategy involving the implementation of the thioalkyl group to boost metabolism, lack of a robust

rat IVIVC caused some concern in relation to the confidence in human  $\text{CL}_b$  projections. Although urinary excretion of unchanged parent was insignificant (< 1% of the dose), the detection of acyl glucuronide conjugates (**22**-acyl glucuronide,  $\text{MH}^+ = 684$ ; **23**-acyl glucuronide,  $\text{MH}^+ = 702$ ) in rat urine indicated glucuronidation as an additional route of elimination, which may explain the weak IVIVC in the rat. The likelihood that HLM  $\text{CL}_b$  values will underpredict in vivo  $\text{CL}_b$  of **22** and **23** in humans is high since in vitro metabolism studies in human hepatocytes also demonstrated the presence of the acyl glucuronide metabolites of **22** and **23**, in addition to the *S*-oxidation products detected in HLM incubations. The inability of in vitro systems to accurately predict glucuronidation-mediated clearance confounds our HLM  $\text{CL}_b$  predictions to a certain degree, and ultimate resolution of the issue will occur in the first in-human PK study. It is of interest to note that despite the high rat

clearances noted with **22** and **23**, the compounds were sufficiently exposed after oral (po) administration as suspensions in methyl cellulose ( $F = 25\text{--}28\%$  at the 10 mg/kg dose; see Table 2).

Endogenous PTH stimulatory effects were evaluated in rats following iv and po administration. Administration of a single iv dose (1 mg/kg) of **22** or **23** resulted in rapid stimulation (within 2 min postdose) of plasma PTH with peak concentrations of 1106 and 979 pg/mL, respectively, which were approximately 8–10-fold higher than basal levels of the hormone in vehicle-treated animals. Oral administration of **22** and **23** at doses of 1, 3, 10, 30, and 100 mg/kg (suspensions in 0.5% methyl cellulose) produced high levels of PTH secretion in a dose-dependent manner. A representative PK/PD effect plot for **22** is depicted in Figure 3. Plasma PTH reached  $t_{\max}$  at 15 min postadministration for all dose groups; associated free  $C_{\max}$  values for **22** and **23** at these doses ranged from 0.3 to 89 nM. The free  $C_{\max}$  values of 14 and 9.7 nM for **22** and **23**, respectively, at the 10 mg/kg dose that provided a robust PTH response provided adequate coverage of the in vitro CaSR  $IC_{50}$ . Consistent with the short effective  $t_{1/2}$  values of **22** and **23**, plasma PTH elevation was

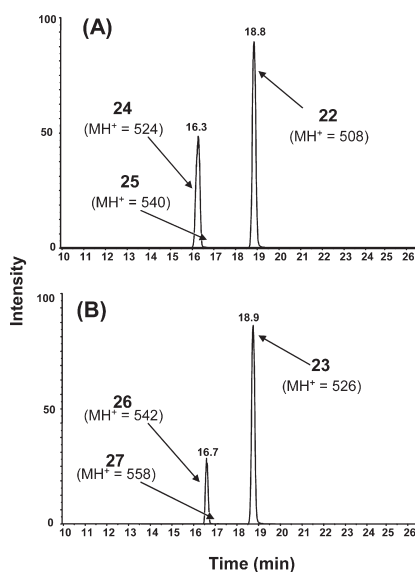


**Figure 2.** Extracted ion chromatogram of NADPH-supplemented HLM incubations of **22** (A) and **23** (B).

**Table 2.** Rat PK Data for CaSR Antagonists Ronacaleret, **3**, **22**, and **23**<sup>a</sup>

compd	dose (mg/kg)	route	RLM $CL_b$	$C_{\max}$ (ng/mL)	$t_{\max}$ (h)	$CL_b$ (mL/min/kg) <sup>d</sup>	$Vd_{ss}$ (L/kg)	$t_{1/2}$ (h) <sup>e</sup>	$F$ (%)
ronacaleret	1	iv	13						
	10	po <sup>b</sup>		136	0.4	62	6.0	2.0	12
<b>3</b>	1	iv	8.7						
	10	po <sup>c</sup>		1980 ± 381	0.7 ± 0.3	25	0.6	2.1	50
<b>22</b>	1	iv	30						
	10	po <sup>c</sup>		273 ± 71	0.5 ± 0.0	75	2.1	0.44	25
<b>23</b>	1	iv	20						
	10	po <sup>c</sup>		658 ± 99.6	0.5 ± 0.0	85	1.1	0.41	28

<sup>a</sup> PK studies were conducted in male Sprague–Dawley rats ( $n = 2\text{--}5$ ). Compounds were administered in glycerol formal containing 2% DMSO (iv) or as suspensions in 0.5% methyl cellulose (po). <sup>b</sup> Administered as the hydrochloride salt ( $n = 2$ ). <sup>c</sup> Administered in free base form. <sup>d</sup>  $CL_b$  values were obtained from plasma clearance divided by the blood partitioning ratio. <sup>e</sup> Half-life values represent the terminal elimination ( $\beta$ ) phase.

transient and returned to levels that were not significantly higher than baseline within 60–120 min postdose.

In summary, we have improved upon the CaSR pharmacology and human PK profile of the lead chemical matter (e.g., compounds **1–3**) with **22** and **23**, respectively. Several attractive features of **22** and **23** also emerged in the course of detailed profiling of their disposition characteristics. For instance, lack of competitive or time-dependent inhibition of CYP3A4 activity in HLM ( $IC_{50} > 30 \mu\text{M}$ ) by **22** and **23** indicates a low risk of nonlinear PK and/or PK interactions with CYP3A4 substrates. Drug–drug interactions via CYP2D6 inhibition by **22** and **23** are also deemed unlikely, given the low predicted human plasma concentrations (unbound  $C_{\max} \sim 25\text{--}34 \text{ nM}$ ) at efficacious doses. Furthermore, weak inhibitory effects on the organic anion transporting polypeptide 1B1 by **22** ( $IC_{50} = 13 \mu\text{M}$ ) and **23** ( $IC_{50} = 40 \mu\text{M}$ )

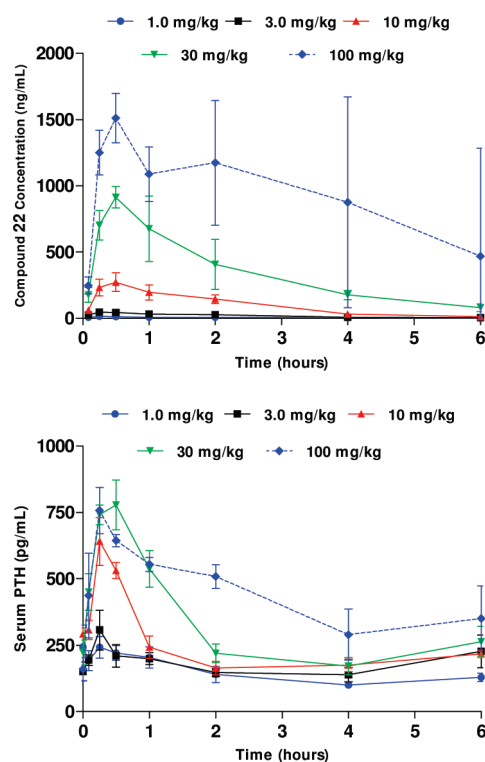


**Figure 3.** Mean PK/PD profile of **22** following po dosing in the Sprague–Dawley rat ( $n = 4/\text{dose}$ ).



mitigate the likelihood of PK interactions with statins, many of which are substrates for hepatic uptake by this transporter.<sup>15</sup> Furthermore, with the involvement of multiple elimination mechanisms (e.g., CYP3A4 oxidation and glucuronidation) for **22** and **23**, the fraction of drug metabolized via a single clearance pathway is reduced and so is the potential for PK interactions involving that pathway. From a drug safety perspective, no clinical signs or histological changes were noted with **22** and **23** in subchronic toxicity testing in rats and dogs at oral doses of 5, 50, and 500 mg/kg. Furthermore, **22** and **23** were devoid of mutagenic responses in the *Salmonella* Ames assay. The necessity for additional safety testing of metabolites<sup>17</sup> is deemed unlikely since no human specific metabolites were detected in in vitro metabolism studies. On the basis of in vitro potency, in vivo oral efficacy, safety, and favorable human disposition attributes, compounds **22** and **23** were selected as clinical candidates for the treatment of osteoporosis.

**SUPPORTING INFORMATION AVAILABLE** Experimental details for the synthesis and characterization of CaSR antagonists **22** and **23** and their primary metabolites, respectively; protocols for in vitro and in vivo pharmacology and disposition studies; and representative LC-MS/MS spectral data from metabolism studies. This material is available free of charge via the Internet at <http://pubs.acs.org>.

#### AUTHOR INFORMATION

**Corresponding Author:** \*To whom correspondence should be addressed. Tel: 860-715-2433. Fax: 860-441-1128. E-mail: amit.kalgutkar@pfizer.com.

#### REFERENCES

- Berry, S. D.; Kiel, D. P.; Donaldson, M. G.; Cummings, S. R.; Kanis, J. A.; Johansson, H.; Samelson, E. J. Application of the National Osteoporosis Foundation Guidelines to Postmenopausal Women and Men: The Framingham Osteoporosis Study. *Osteoporosis Int.* **2010**, *21* (1), 53–60.
- File, E.; Deal, C. Clinical Update on Teriparatide. *Curr. Rheumatol. Rep.* **2009**, *11* (3), 169–176.
- Garrett, J. E.; Capuano, I. V.; Hammerland, L. G.; Hung, B. C.; Brown, E. M.; Hebert, S. C.; Nemeth, E. F.; Fuller, F. Molecular Cloning and Functional Expression of Human Parathyroid Calcium Receptor cDNAs. *J. Biol. Chem.* **1995**, *270* (21), 12919–12925.
- Gowen, M.; Stroup, G. B.; Dodds, R. A.; James, I. E.; Votta, B. J.; Smith, B. R.; Bhatnagar, P. K.; Lago, A. M.; Callahan, J. F.; Delmar, E. G.; Miller, M. A.; Nemeth, E. F.; Fox, J. Antagonizing the Parathyroid Calcium Receptor Stimulates Parathyroid Hormone Secretion and Bone Formation in Osteopenic Rats. *J. Clin. Invest.* **2000**, *105* (11), 1595–1604.
- Nemeth, E. F.; Delmar, E. G.; Heaton, W. L.; Miller, M. A.; Lambert, L. D.; Conklin, R. L.; Gowen, M.; Gleason, J. G.; Bhatnagar, P. K.; Fox, J. Calcilytic Compounds: Potent and Selective Ca<sup>2+</sup> Receptor Antagonists That Stimulate Secretion of Parathyroid Hormone. *J. Pharmacol. Exp. Ther.* **2001**, *299* (1), 323–331.
- Didiuk, M. T.; Griffith, D. A.; Benbow, J. W.; Liu, K. K.; Walker, D. P.; Bi, F. C.; Morris, J.; Guzman-Perez, A.; Gao, H.; Bechle, B. M.; Kelley, R. M.; Yang, X.; Dirico, K.; Ahmed, S.; Hungerford, W.; DiBrinno, J.; Zawistoski, M. P.; Bagley, S. W.; Li, J.; Zeng, Y.; Santucci, S.; Oliver, R.; Corbett, M.; Olson, T.; Chen, C.; Li, M.; Paralkar, V. M.; Riccardi, K. A.; Healy, D. R.; Kalgutkar, A. S.; Maurer, T. S.; Nguyen, H. T.; Frederick, K. S. Short-Acting 5-(Trifluoromethyl)pyrido[4,3-d]pyrimidin-4(3H)-one Derivatives as Orally-Active Calcium-Sensing Receptor Antagonists. *Bioorg. Med. Chem. Lett.* **2009**, *19* (16), 4555–4559.
- Gavai, A. V.; Vaz, R. J.; Mikkilineni, A. B.; Roberge, J. Y.; Liu, Y.; Lawrence, R. M.; Corte, J. R.; Yang, W.; Bednarz, M.; Dickson, J. K., Jr.; Ma, Z.; Seethala, R.; Feyen, J. H. Discovery of Novel 1-Arylmethyl Pyrrolidin-2-yl Ethanol Amines as Calcium-Sensing Receptor Antagonists. *Bioorg. Med. Chem. Lett.* **2005**, *15* (24), 5478–5482.
- Balan, G.; Bauman, J.; Bhattacharya, S.; Castrodad, M.; Healy, D. R.; Herr, M.; Humphries, P.; Jennings, S.; Kalgutkar, A. S.; Kapinos, B.; Khot, V.; Lazarra, K.; Li, M.; Li, Y.; Neagu, C.; Oliver, R.; Piotrowski, D. W.; Price, D.; Qi, H.; Simmons, H. A.; Southers, J.; Wei, L.; Zhang, Y.; Paralkar, V. M. The Discovery of Novel Calcium Sensing Receptor Negative Allosteric Modulators. *Bioorg. Med. Chem. Lett.* **2009**, *19* (12), 3328–3332.
- Marquis, R. W.; Lago, A. M.; Callahan, J. F.; Rahman, A.; Dong, X.; Stroup, G. B.; Hoffman, S.; Gowen, M.; DelMar, E. G.; Van Wagenen, B. C.; Logan, S.; Shimizu, S.; Fox, J.; Nemeth, E. F.; Roethke, T.; Smith, B. R.; Ward, K. W.; Bhatnagar, P. Antagonists of the Calcium Receptor. 2. Amino Alcohol-Based Parathyroid Hormone Secretagogues. *J. Med. Chem.* **2009**, *52* (21), 6599–6605.
- Deal, C. Potential New Drug Targets for Osteoporosis. *Nature Clin. Pract. Rheumatol.* **2009**, *5* (1), 20–27.
- Fukumoto, S.; Nakamura, T.; Nishizawa, Y.; Hayashi, M.; Matsumoto, T. Randomized, Single-Blinded Placebo-Controlled Study of a Novel Calcilytic, JTT-505, in Patients with Postmenopausal Osteoporosis. *ASBMR Abstract 1131*.
- Shinagawa, Y.; Inoue, T.; Kiguchi, T.; Ikenogami, T.; Ogawa, N.; Fukuda, K.; Nakagawa, T.; Shindo, M.; Soejima, Y. Preparation of Arylcarboxylic Acid Derivatives as CaSR Antagonists. WO 2004/094362.
- Middleton, D. S.; Andrews, M.; Glossop, P.; Gymer, G.; Hepworth, D.; Jessiman, A.; Johnson, P. S.; MacKenny, M.; Stobie, A.; Tang, K.; Morgan, P.; Jones, B. Designing Rapid Onset Selective Serotonin Re-uptake Inhibitors. Part 3: Site-Directed Metabolism as a Strategy To Avoid Active Circulating Metabolites: Structure-Activity Relationships of (Thioalkyl)phenoxy Benzyl Amines. *Bioorg. Med. Chem. Lett.* **2008**, *18* (19), 5303–5306.
- Obach, R. S. Prediction of Human Clearance of Twenty-Nine Drugs from Hepatic Microsomal Intrinsic Clearance Data: An Examination of in Vitro Half-Life Approach and Nonspecific Binding to Microsomes. *Drug Metab. Dispos.* **1999**, *27* (11), 1350–1359.
- Kalliokoski, A.; Niemi, M. Impact of OATP Transporters on Pharmacokinetics. *Br. J. Pharmacol.* **2009**, *158* (3), 693–705.
- Brown, H. C.; Ramachandran, V. Asymmetric Reduction with Chiral Organoboranes Based on  $\alpha$ -Pinene. *Acc. Chem. Res.* **1992**, *25* (1), 16–24.
- Smith, D. A.; Obach, R. S. Metabolites in Safety Testing (MIST): Considerations of Mechanisms of Toxicity with Dose, Abundance, and Duration of Treatment. *Chem. Res. Toxicol.* **2009**, *22* (2), 267–279.